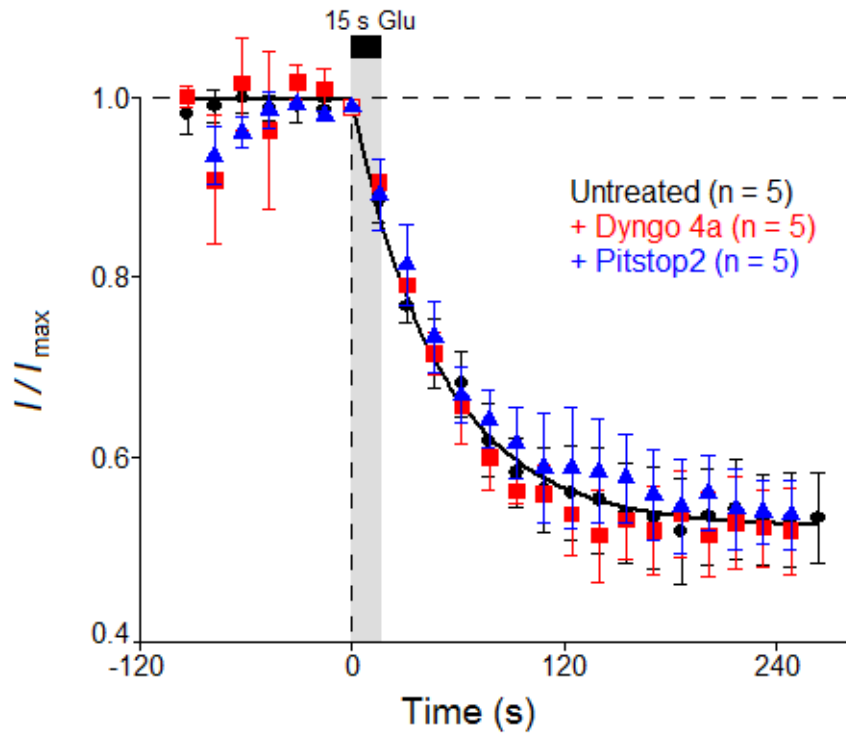


## SUPPLEMENTAL INFORMATION

There are seven Supplemental Figures with their Legends, Supplemental Experimental Procedures, and Supplemental References.

### SUPPLEMENTAL FIGURES and FIGURE LEGENDS



**Figure S1. Related to Figure 1. Inhibitors of clathrin-mediated endocytosis do not prevent glutamate-mediated inhibition of neuronal L current.**

In cultured hippocampal neurons (4-5 DIV), peak inward  $Ca^{2+}$  currents were elicited by steps once every 15 s to 0 mV (500 ms duration) from a holding potential of  $-60$  mV. Starting at time 0, 100  $\mu$ M glutamate + 1  $\mu$ M glycine was applied to the recorded neuron for 15 s, using the fast perfusion system described in the Experimental Procedures. Pitstop2 (Abcam #ab120687) or Dyngo 4a (Abcam #ab120689) was included in the whole patch pipet solution at 30  $\mu$ M and 10  $\mu$ M, respectively.

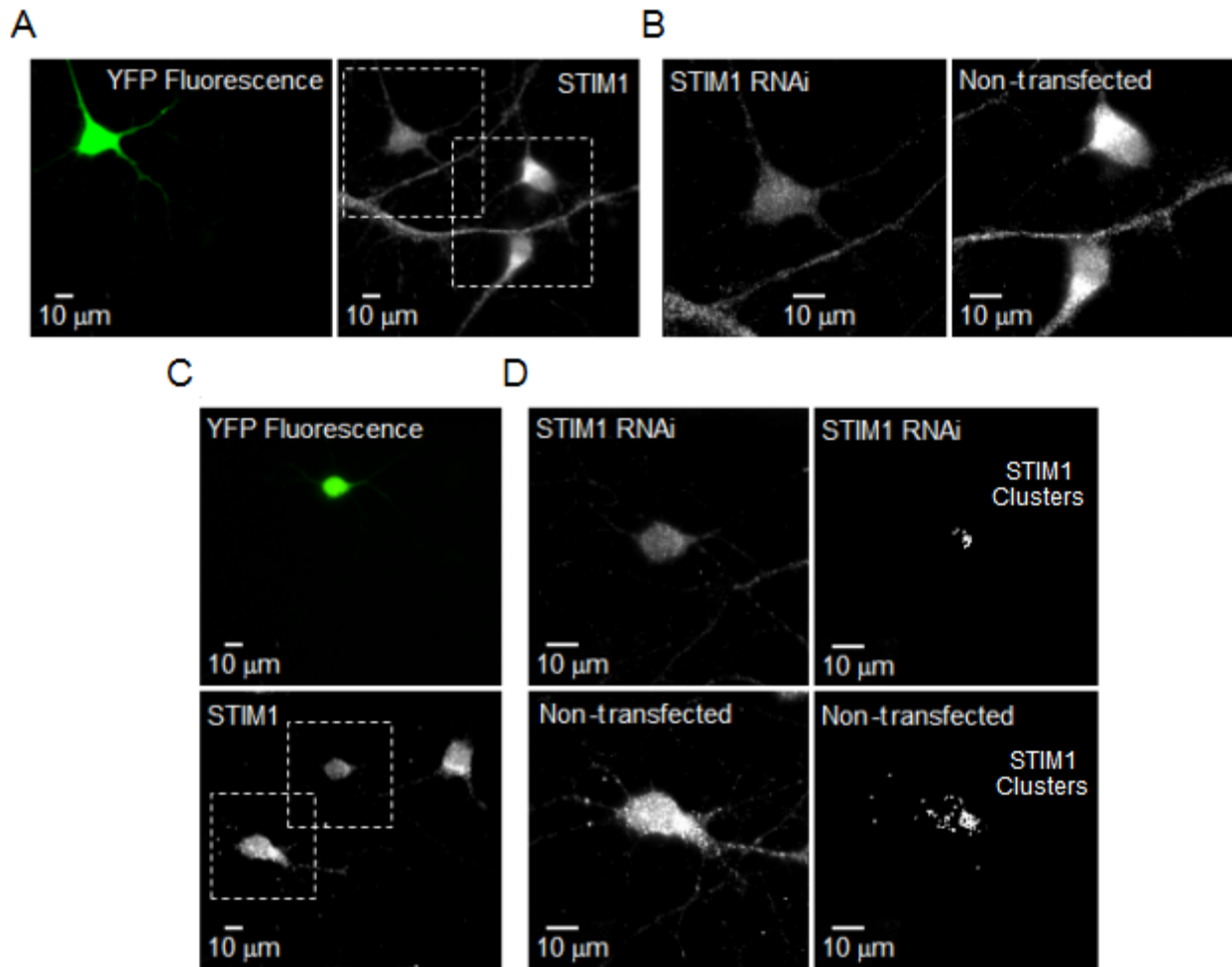


**Figure S2. Related to Figure 1. STIM1 RNAi significantly reduced both STIM1 expression and clustering in hippocampal neurons.**

(A) YFP fluorescence (left) identified neurons transfected with STIM1 RNAi + YFP. Immunostaining for STIM1 (right; Alexa-647) in transfected and non-transfected neurons.

(B) Enlarged projection images constructed from z-stacks (200 nm steps) of neurons, as indicated by the dashed white boxes in the right-hand panel of (A). Comparison of Alexa-647 fluorescence intensity in a YFP-positive neuron expressing the STIM1 RNAi construct (left) with Alexa-647 intensity in YFP-negative, non-transfected neurons (right) demonstrated a reduction in STIM1 expression in the STIM1 RNAi neuron.

(C) Neurons were treated with thapsigargin (2  $\mu$ M) to deplete ER  $Ca^{2+}$ . YFP fluorescence (top) identifies a neuron transfected with STIM1 RNAi + YFP. STIM1 (bottom) was identified by immunostaining in transfected and non-transfected neurons.

(D) Enlarged immunofluorescence image of a neuron expressing the STIM1 RNAi (top, left) compared to enlarged immunofluorescence image of a non-transfected neuron (bottom, left) revealed a relative reduction in STIM1 clustering in the STIM1 RNAi neuron. White dashed boxes in c indicate the regions enlarged in (D). In the right-hand panels, STIM1 clusters identified using the particle analysis tool in Fiji are presented: identified STIM1 clusters in a neuron expressing STIM1 RNAi are displayed at top, right, and identified STIM1 clusters in a non-transfected neuron are displayed at bottom, right. Neurons: 4-5 DIV.

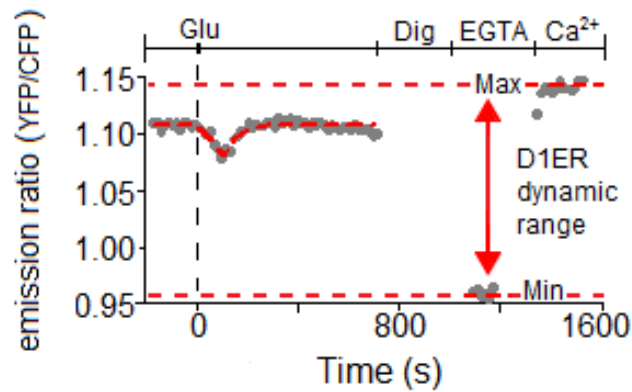


**Figure S3. Related to Figure 1. Calibration of the D1ER Ca<sup>2+</sup> sensor in hippocampal neurons.**

At the end of each experiment measuring  $[Ca^{2+}]_{ER}$  responses to bath applied glutamate, the neuron under study was stimulated by 15 s bath application of 100  $\mu$ M glutamate + 1  $\mu$ M glycine and then permeabilized by treatment with 15  $\mu$ M digitonin for 2 min. The neuron was subsequently bathed in a solution lacking added Ca<sup>2+</sup> and containing 1 mM EGTA, and the minimum D1ER response was determined from the ratio of YFP and CFP emission (from the D1ER sensor) under these conditions. Finally, the maximum response of D1ER to Ca<sup>2+</sup> was determined by bathing the permeabilized neuron in a solution containing 40 mM Ca<sup>2+</sup> and 20 mM Ba<sup>2+</sup>. Neurons: 4-5 DIV.

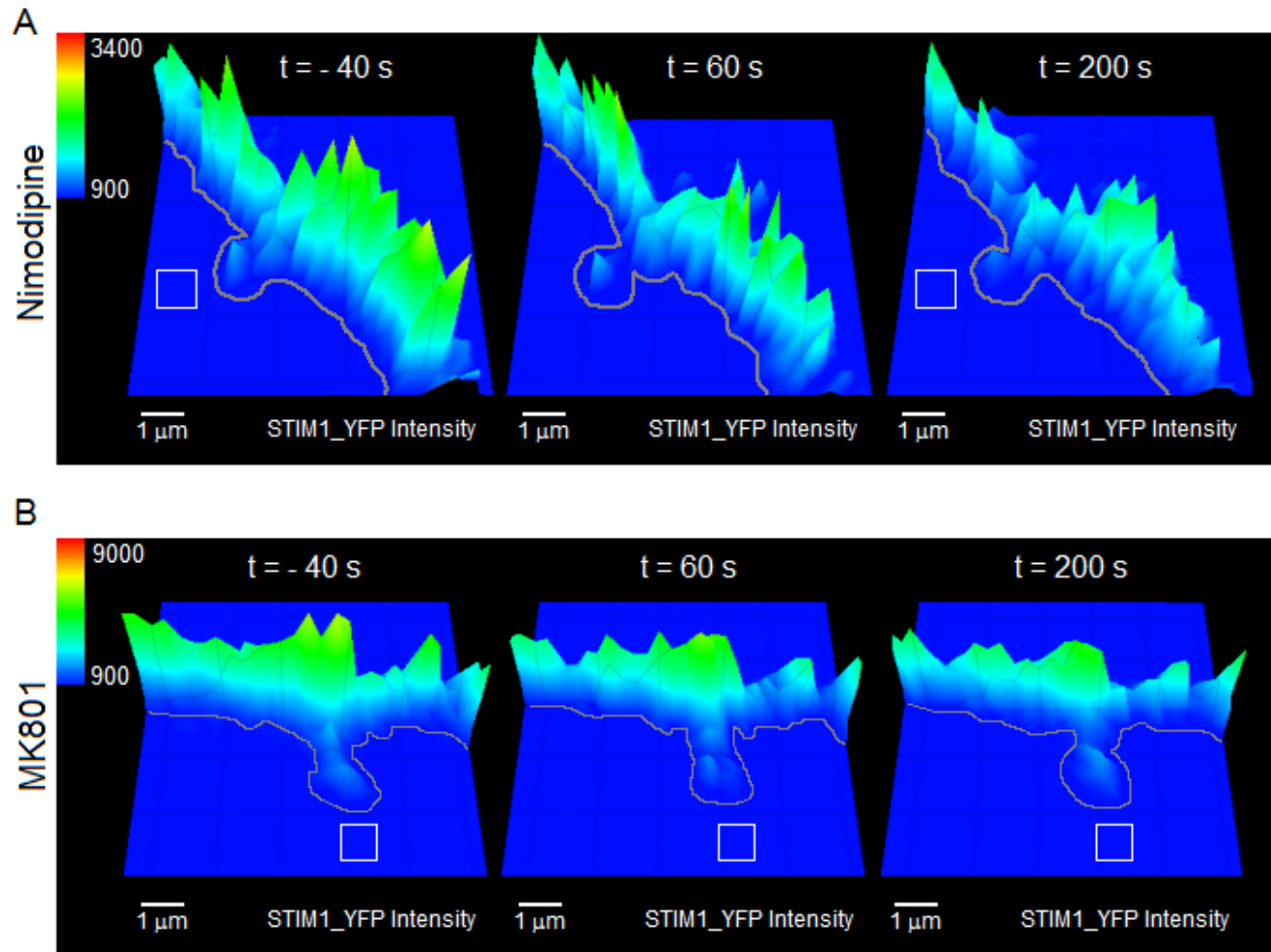


**Figure S4. Related to Figure 2. Block of NMDARs with MK801 or of LTCCs with nimodipine prevents glutamate uncaging-driven increases in STIM1-YFP clustering.**

YFP intensity plots derived from confocal images illustrate lack of clustering of STIM1-YFP in response to uncaging of glutamate (2 mM MNI-glutamate + 1 μM glycine in bath) in neurons bathed in (A) nimodipine (5 μM) or (B) MK801 (10 μM). Uncaging protocol: 2 ms laser pulses once per second, for 60 s starting at time = 0 s. White box indicates uncaging region. Neurons: 12-14 DIV.

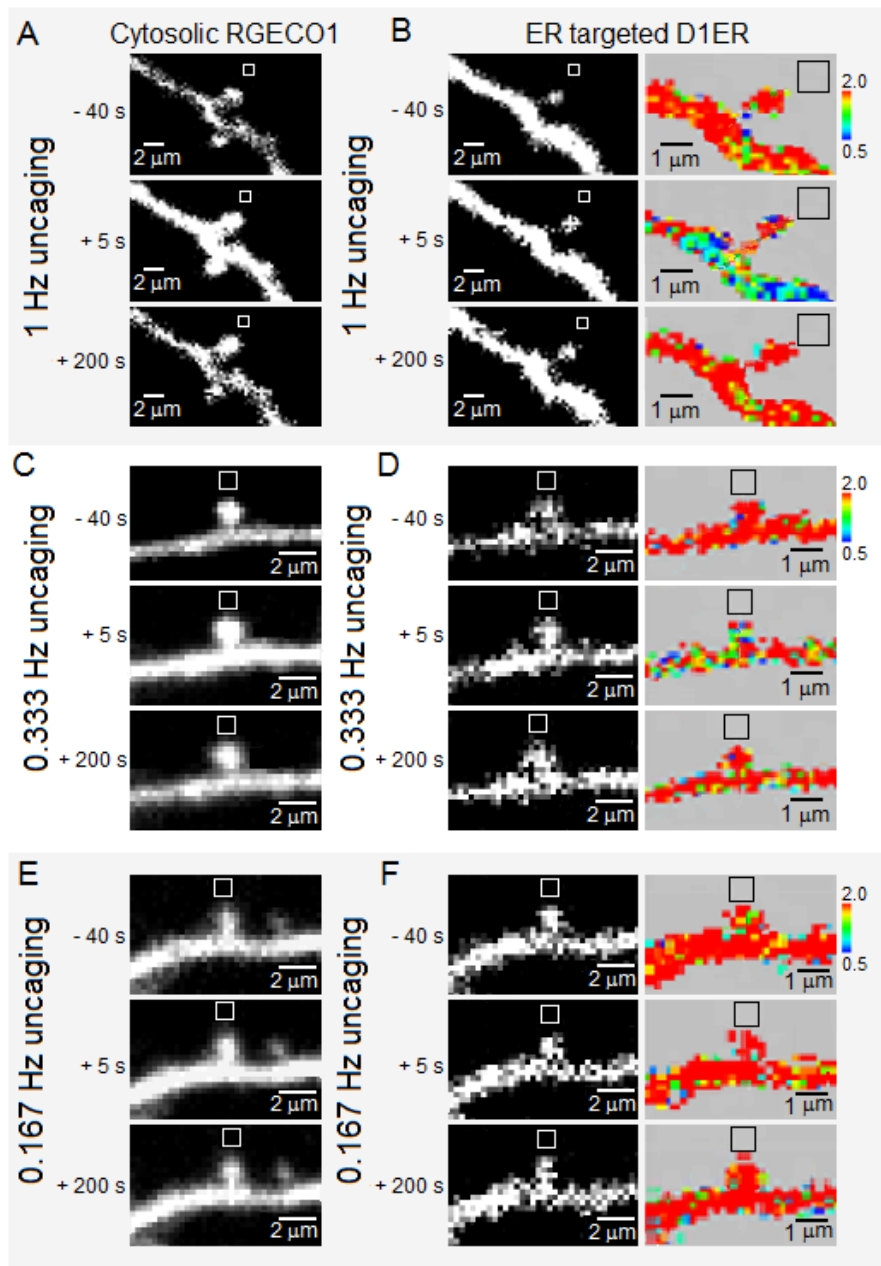


**Figure S5. Related to Figure 4. Images of dendrites illustrating the frequency dependence of L channel-dependent changes in cytosolic  $\text{Ca}^{2+}$  and ER  $\text{Ca}^{2+}$ .**

In 12-14 DIV neurons expressing both RGECO1 and D1ER, simultaneous imaging of  $[\text{Ca}^{2+}]_{\text{cyto}}$  and  $[\text{Ca}^{2+}]_{\text{ER}}$  was carried out at three different stimulation frequencies: 1 Hz, 0.333 Hz and 0.167 Hz. MNI-glutamate (2 mM) was uncaged with 2 ms flashes of 405 nm laser illumination applied near a spine (square white box). Bath contained 1  $\mu\text{M}$  glycine, 3 mM  $\text{CaCl}_2$  and 0  $\text{Mg}^{2+}$ . (A, C and E) Dendritic shaft with spines imaged by collecting RGECO1 fluorescence before, during and after glutamate uncaging. Initial RGECO1 intensity (-40 s) was low in all three panels. By 5 s after the onset of uncaging, RGECO1 intensity was high for the 1 Hz uncaging train; intensity was not as high for the 0.333 Hz train, and little to no increase in RGECO1 intensity was observed at 0.167 Hz uncaging. Fluorescence returned to pre-uncaging levels by 200 s after the onset (140 s after the end) of the 60 s uncaging trains.

(B, D and F) Black and white image of the same neurons as in (A), (C) and (E), but imaging the citrine moiety of D1ER. On the right, FRET imaging of ER  $\text{Ca}^{2+}$  in these same regions, presented on a pseudocolor scale. By 5 s into the uncaging train,  $[\text{Ca}^{2+}]_{\text{ER}}$  declined the most for 1 Hz uncaging, less for 0.333 Hz uncaging, and little to none at 0.167 Hz uncaging.

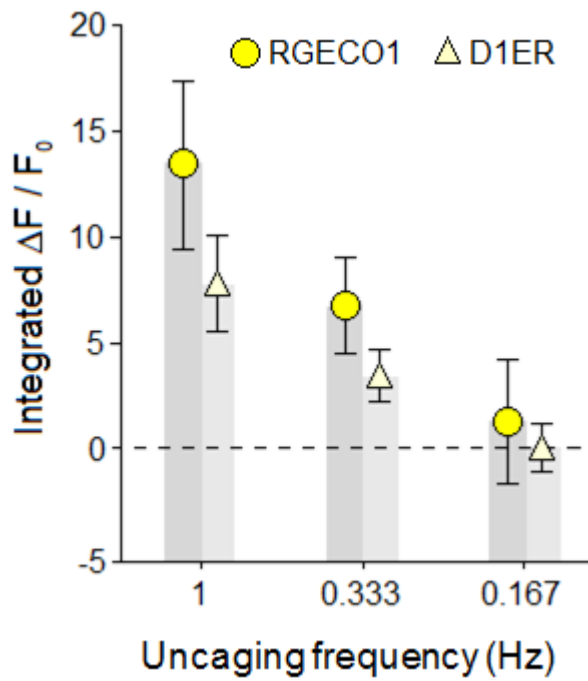


**Figure S6. Related to Figure 4. Co-dependence of LTCC-driven elevation of cytoplasmic  $\text{Ca}^{2+}$  and of ER  $\text{Ca}^{2+}$  upon total “synaptic drive.”** Increasing the number of glutamate uncaging stimuli in a 1 min period from 10 (0.167 Hz), to 20 (0.333 Hz) to 60 (1 Hz) increased the size of the LTCC-dependent component of both  $[\text{Ca}^{2+}]_{\text{cyto}}$  and of ER  $\text{Ca}^{2+}$  release.

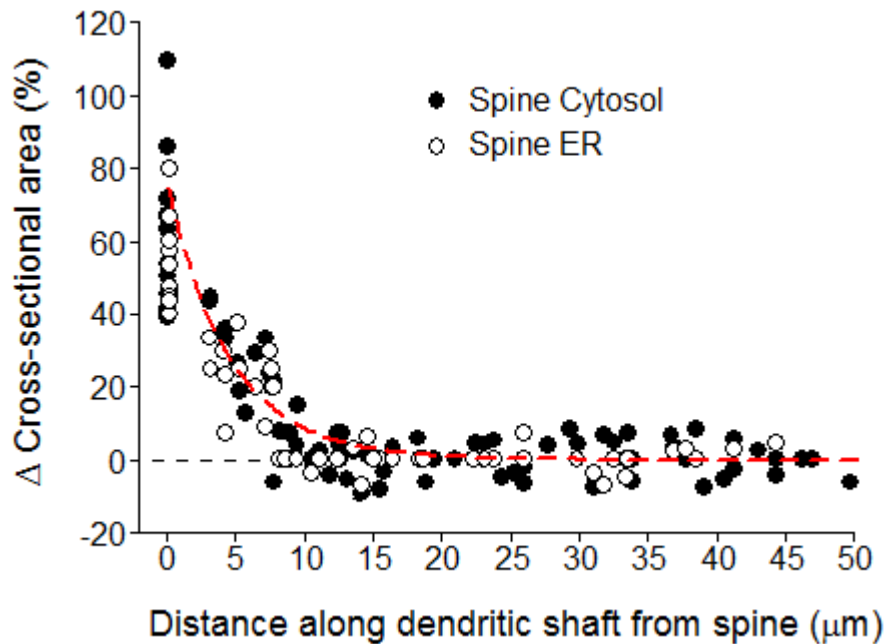


**Figure S7. Related to Figure 6. Growth in cross-sectional area and ER content of spines neighboring a stimulated spine, as a function of the distance along the dendrite from the stimulated spine.** For spine cross-sectional area, a total of  $n = 72$  spines neighboring a stimulated spine was measured. For ER cross-sectional area, a total of  $n = 54$  spines was measured. Cross-sectional areas were measured as for Figure 6. At the stimulated spine: glutamate was uncaged at 1 Hz for 60 s.

## SUPPLEMENTAL EXPERIMENTAL PROCEDURES

### Culture and transfection of primary hippocampal neurons

For 4-5 DIV neurons, transfection was accomplished with an AMAXA Nucleofector protocol: dissociated neurons were centrifuged, resuspended at  $3.5 \times 10^6 - 4 \times 10^6$  cells/transfection in AMAXA buffer, electroporated with 6-8  $\mu\text{g}$  of total DNA, and plated at  $6 \times 10^5 - 8 \times 10^5$  cells per poly-D-lysine coated glass coverslip (25 mm diameter). Neurons were plated in glutamine-supplemented Minimum Essential Medium (MEM) plus fetal bovine serum, and 4 hrs after plating, the medium was replaced with fresh medium. After one day, MEM was replaced with B27-supplemented Neurobasal-A medium.

For cultures studied at 12-16 DIV, neurons were plated at  $3 \times 10^5 - 4 \times 10^5$  cells per glass coverslip, maintained for up to 16 DIV in B27-supplemented Neurobasal-A, and neurons were fed every 4-5 days with fresh medium that, after the first 4-5 days in culture, contained mitotic inhibitors. These longer-term neuron cultures were transfected 2 days prior to imaging, using Lipofectamine 2000 reagent (Invitrogen) and 2  $\mu\text{g}$  of each cDNA used in a particular experiment.

### Constructs

Human STIM1 fused at its C terminal to YFP or CFP were gifts from Anjana Rao (Addgene plasmids #19754 and #19755) (Prakriya et al., 2006). D1ER was a gift from Amy Palmer (Addgene plasmid #36325) (Palmer et al., 2004). RGECO1 and RGECO1a were gifts from Robert Campbell and Douglas Kim, respectively (Addgene plasmids #32444 and # 61563) (Dana et al., 2016; Zhao et al., 2011). Rabbit  $\text{Ca}_v1.2$  fused at its N terminal to CFP was a gift from Kurt Beam (University of Colorado School of Medicine). The pcDNA3-GFP-NFATc3 construct consisted of GFP fused to the N-terminus of human NFAT (3-2098) and an artificial sequence (GTACGAGGAGTCATGATGGTTTACTA) fused at the C-terminus (Murphy et al., 2014). The sGFP2-NFATc3 construct was generated by excising NFATc3 and the artificial C terminal sequence with HindIII and ApaI restriction sites and then ligating this into the pSGFP2-C1 vector (Addgene plasmid #22881; gift from Dorus Gadella) (Kremers et al., 2007) between the HindIII and ApaI sites.

### Patch-clamp recording

On the stage of the recording microscope, transfected neurons were identified by fluorescence from YFP, or by fluorescently-tagged STIM1 constructs.  $\text{Ca}^{2+}$  currents were voltage-clamped using patch pipets of 3-5 M $\Omega$  resistance and an Axopatch 200A amplifier (Molecular Devices). Series resistance compensation, capacitance cancellation, and leak subtraction were employed. Current records were low-pass filtered at 2 kHz, and sampled at 10 kHz using PatchMaster software (HEKA). Only recordings with an access resistance <10 M $\Omega$  were pursued.

### RNAi knockdown of STIM1

Endogenous rat STIM1 was knocked down in neurons using plasmid-based RNA interference (RNAi). The short hairpin RNAi was generated by ligating a sequence targeting STIM1 (994-1014) between the HindIII and EcoRI restriction sites in a pSilencer vector (Ambion, Austin, TX). The primers were based on the short hairpin RNAi sequence described by Park et al. (2010): forward, 5'-AGCTTCAGAAGGAGCTGGAATCACACTTCAAGAGAGTGTGATTCCAGCTCCTTCTTTTTTACGCGTG-3'; and reverse, 5'-ATTCACGCGTAAAAAAGAAGGAGCTGGAATCACACTCTCTTGAAGTGTGATTCCAGCTCCTTCTGA-3'. At 2-3 days after transfection of the plasmid, total STIM1 levels were reduced to  $36.7 \pm 8.7\%$  ( $n = 8$ ; measured by anti-STIM1 immunofluorescence intensity in projection images constructed from digitally-deconvolved z-stacks; **Figure S2**) and the number of STIM1 clusters was reduced to  $22.2 \pm 10.6\%$  ( $n = 5$ ) (**Figure S2**). Human STIM1 was insensitive to rat STIM1RNAi, as was hSTIM(D76A) (alanine substitution for aspartate in the  $\text{Ca}^{2+}$ -binding luminal EF hand, at residue 76).

### Immunofluorescence analysis of RNAi knockdown of STIM1

For immunofluorescence measurements in **Figure S1**, fluorescence images were acquired from cultured rat neurons (4-5 DIV) transfected with anti-rat STIM1RNAi using a Zeiss Axiovert 200M inverted fluorescence microscope equipped with a 175 W xenon illumination source,  $\alpha$  Plan-Apochromat 100x (1.40 NA) oil-immersion objective lens, CoolSNAP HQ CCD camera with 12-bit dynamic range (Photometrics), and dual filter wheels (Sutter Instruments) controlled by SlideBook 5.0 software (Intelligent Imaging Innovations). Fixed neurons were stained with a STIM1 (D88E10) rabbit monoclonal antibody (Cell Signaling Technology Cat# 5668S RRID:AB\_10828699) and an Alexa Fluor 647-conjugated goat anti-rabbit antibody (Invitrogen).

Fluorescence images were captured using an exposure time of 50-100 ms, and a Cy5 filter set: 645/30 nm excitation; 660/40 nm emission. Image analysis was performed using the add-on tools available in 64-bit Fiji software (Schindelin et al., 2012).

### Measurement of $[Ca^{2+}]_{ER}$ with D1ER

To measure  $[Ca^{2+}]_{ER}$ , donor (CFP) and raw FRET images were captured using an exposure time of 200-400 ms, and filter sets for donor (CFP; 436/10 nm excitation, 470/30 nm emission) and raw FRET (*rawFRET*; 436/10 nm excitation, 535/30 nm emission). For each selected region of interest (ROI), the FRET ratio ( $R$ ) was calculated from background-corrected (BKG) raw FRET and CFP fluorescence image intensities (INT) as

$$R = (FRET_{INT} - FRET_{BKG}) / (CFP_{INT} - CFP_{BKG}).$$

Background ROIs were selected from non-transfected neurons. D1ER FRET ratios were converted to percent maximum FRET ratio as

$$\% \Delta R = (R - R_{min}) / (R_{max} - R) \times 100$$

and to  $[Ca^{2+}]$  by solving the equation

$$\% \Delta R = \{ R_{max1} \cdot [Ca^{2+}]^{n1} / (K_{D1}^{n1} + [Ca^{2+}]^{n1}) \} + \{ R_{max2} \cdot [Ca^{2+}]^{n2} / (K_{D2}^{n2} + [Ca^{2+}]^{n2}) \}$$

where  $K_{D1} = 0.58 \mu M$ ,  $K_{D2} = 56.46 \mu M$ ,  $R_{max1} = 0.28$ ,  $R_{max2} = 0.72$ ,  $n1 = 1.18$ , and  $n2 = 1.67$  (Palmer et al., 2004).  $R_{min}$  and  $R_{max}$  were determined at the end of each experiment by permeabilizing the neuron with 15  $\mu M$  digitonin (2 min treatment):  $R_{min}$  was determined in a bath solution lacking added  $Ca^{2+}$  and containing 1 mM EGTA, and  $R_{max}$  was determined in a bath solution containing 40 mM  $Ca^{2+}$  and 20 mM  $Ba^{2+}$ .

### Total internal reflection fluorescence (TIRF) microscopy

Fluorescence images were acquired from cultured neurons (12-14 DIV) transfected with STIM1-YFP or STIM1(D76A)-YFP using a Zeiss Elyra P.1 imaging system based on an Axio Observer Z1 inverted fluorescence microscope equipped with an  $\alpha$  Plan-Apochromat 100x (1.46 NA) oil-immersion objective lens; a 488 nm/200 mW optically-pumped semiconductor laser; an Andor iXon 897 EMCCD camera with 16-bit dynamic range; and was controlled by ZEN 2012 software (Zeiss). TIRF images of STIM1-YFP were captured using a dichroic mirror (405/488/561/642 nm) and an emission filter with a band pass of 495-575 nm and >750 nm. Analysis was performed using 64-bit Fiji software.

### Photo-uncaging MNI-glutamate and simultaneous imaging of $[Ca^{2+}]_{cyto}$ and $[Ca^{2+}]_{ER}$

Images in the *RFP* channel (for RGECO1) and in the *CFP* and *FRET* channels (for D1ER) were collected every second for the duration of the experiment. To calculate  $[Ca^{2+}]_{cyto}$ ,  $\Delta F/F_0$  values were calculated by subtracting the average RGECO1 intensity (*RFP* channel) prior to glutamate uncaging ( $F_0$ ) from background-corrected RGECO1 intensity at subsequent times, and normalizing to  $F_0$ . For D1ER FRET, FRET ratios ( $R$ ) were calculated from background-corrected FRET and CFP fluorescence images, and normalized to  $R_0$  (initial  $R$ , prior to glutamate).

### FRET between STIM1-YFP and CFP-Ca $\nu$ 1.2

Light that passed through the FRET filter set was contaminated by donor bleed-through (average fraction, 0.24) and acceptor cross-excitation (average fraction, 0.032); fractional contamination by bleed-through and cross-excitation were determined in separate experiments using cells that expressed CFP- or YFP-tagged constructs alone. Corrected, sensitized FRET ( $FRET^C$ ) images were obtained by subtracting the contamination components, pixel by pixel, from raw FRET images using the following equation:  $FRET^C = rawFRET - (0.24 * CFP) - (0.032 * YFP)$ . Sensitized  $FRET^C$  images were generated using SlideBook 6.0 software (Intelligent Imaging Innovations). FRET ratios ( $R$ ) were calculated from background-corrected FRET and YFP fluorescence images, and normalized to  $R_0$  (initial  $R$ , prior to glutamate).



### **Measurement of spine and ER cross-sectional areas**

For measurement of cross-sectional areas of dendritic spines, RGECO1 was used as a reporter of cytosolic area. RGECO1 emission was captured in the *RFP* channel (561 nm excitation; 617/73 nm emission). For measurement of cross-sectional areas of spine ER compartments, D1ER was used as a reporter of ER area. For this purpose, emission from the citrine moiety of D1ER was captured in the *YFP* channel (515 nm excitation; 525/50 nm emission). For both channels, regions outlining the fluorescence intensity (whole spine or spine ER) were drawn on images collected prior to glutamate uncaging. Outlined regions were converted to masks and each mask was analyzed using Slidebook 6.0 to extract cross-sectional areas. For images collected 200 s after the first laser uncaging pulse (140 s after the end of stimulation), the same spines were again analyzed by outlining regions of RGECO1 or D1ER-citrine fluorescence, outlined regions were converted to masks, and cross-sectional areas for the masks were obtained.

### **NFATc3 translocation assay for 15 s bath application of glutamate**

Incubations in TTX, both before and after glutamate, were carried out using a bath solution identical to that employed for patch clamp recording, and maintained at 37°C. Glutamate stimulation (15 s) was carried out at room temperature, in TTX-free patch clamp bath solution. For pharmacological studies, nimodipine (5 µM) or MK801 (10 µM) was included in the TTX-supplemented solution for 30 min prior to glutamate stimulation, and the blocker was also included for the remainder of the protocol, including during stimulation. Fixed neurons were stained with rabbit anti-GFP rabbit antibody (Molecular Probes Cat# A-11122 RRID:AB\_221569) plus Alexa Fluor 488 goat anti-rabbit (Molecular Probes Cat# A-11008 RRID:AB\_143165) and DAPI. To measure intensity of GFP-NFATc3 immunofluorescence, a series of optical sections (0.2 µm steps) along the z-axis was collected from each neuron using the Axiovert 200M-based system described above, the z-stack was digitally deconvolved and a two-dimensional, summed-intensity projection image was used for analysis. Quantitative mask analysis of the projection images was carried out using SlideBook 5.0 to obtain mean immunofluorescence intensities in the nucleus and in the cytoplasm of the neuronal soma.

### **NFATc3 translocation assay for glutamate uncaging**

For pharmacological studies, nimodipine (5 µM) was included in the TTX-supplemented solution for 30 min prior to glutamate treatment, and the blocker was also included for the remainder of the protocol, including during glutamate uncaging. Fluorescence images were acquired using a Zeiss Observer.Z1 inverted microscope equipped with an EC Plan-Neofluar 40x (1.30 NA) oil-immersion objective lens; 405 nm/50 mW, 488 nm/40 mW, 561 nm/50 mW and 640 nm/50 mW lasers; an mSAC unit for correction of spherical aberration (Intelligent Imaging Innovations); a Yokogawa CSU-X1 spinning disk unit; a Photometrics PVCAM (Dynamic) EMCCD camera with 16-bit dynamic range; a Vector live specimen scanner (Intelligent Imaging Innovation) for positioning the photo-uncaging laser; and an mSwitcher ms optical switching unit (Intelligent Imaging Innovation) that enabled simultaneous use of the CSU-X 1 and Vector units. Instrumentation was controlled by SlideBook 6.0 software (Intelligent Imaging Innovation). A dichroic mirror (445/515/640; Semrock) and two different filter sets (*RFP*, 561 nm excitation, 617/73 nm emission; *GFP*, 488 nm excitation, 525/50 nm emission) were used to capture serially pairs of images: a 100 ms exposure for GFP and a 40 ms exposure for RFP. A total of 15 xy image pairs (*RFP* and *GFP*) were collected within a 7 µm z-stack, at 0.5 µm intervals. For uncaging of glutamate, a 1 µm x 1 µm region was selected near a dendritic spine of interest. Glutamate was photo-uncaged from MNI-glutamate in this region using 1 ms pulses from a 405 nm/50 mW laser, according to the following laser pulse pattern: three 20-s bursts of 1-ms laser pulses at applied at 1 Hz within each burst and with a 6 s interburst interval (60 laser pulses total). Z-stack images in the *RFP* channel (for RGECO1a) and in the *GFP* channel (for sGFP2-NFATc3) were collected at -5, -1, 1, 5, 10, 20, 30 and 40 minutes from initiation of glutamate uncaging. To calculate normalized nucleus-to-cytosol ratios, regions of interest (ROI) were drawn around the nucleus, cytosolic area in the neuronal soma, and a background area outside the neuron to determine background-corrected mean sGFP2 fluorescence intensity in the nucleus and cytosol. Nucleus-to-cytosol ratios were calculated from background-corrected nuclear and cytosolic mean fluorescence intensities, and normalized to pre-uncaging values. Analyses of image data were performed using SlideBook 6.0.

## SUPPLEMENTAL REFERENCES

Dana, H., Mohar, B., Sun, Y., Narayan, S., Gordus, A., Hasseman, J.P., Tsegaye, G., Holt, G.T., Hu, A., Walpita, D., *et al.* (2016). Sensitive red protein calcium indicators for imaging neural activity. *eLife* 5.

Kremers, G.J., Goedhart, J., van den Heuvel, D.J., Gerritsen, H.C., and Gadella, T.W., Jr. (2007). Improved green and blue fluorescent proteins for expression in bacteria and mammalian cells. *Biochemistry (Mosc)* 46, 3775-3783.

Murphy, J.G., Sanderson, J.L., Gorski, J.A., Scott, J.D., Catterall, W.A., Sather, W.A., and Dell'Acqua, M.L. (2014). AKAP-anchored PKA maintains neuronal L-type calcium channel activity and NFAT transcriptional signaling. *Cell Rep* 7, 1577-1588.

Palmer, A.E., Jin, C., Reed, J.C., and Tsien, R.Y. (2004). Bcl-2-mediated alterations in endoplasmic reticulum  $Ca^{2+}$  analyzed with an improved genetically encoded fluorescent sensor. *Proc Natl Acad Sci U S A* 101, 17404-17409.

Park, C.Y., Shcheglovitov, A., and Dolmetsch, R. (2010). The CRAC channel activator STIM1 binds and inhibits L-type voltage-gated calcium channels. *Science* 330, 101-105.

Prakriya, M., Feske, S., Gwack, Y., Srikanth, S., Rao, A., and Hogan, P.G. (2006). Orai1 is an essential pore subunit of the CRAC channel. *Nature* 443, 230-233.

Schindelin, J., Arganda-Carreras, I., Frise, E., Kaynig, V., Longair, M., Pietzsch, T., Preibisch, S., Rueden, C., Saalfeld, S., Schmid, B., *et al.* (2012). Fiji: an open-source platform for biological-image analysis. *Nat Methods* 9, 676-682.

Zhao, Y., Araki, S., Wu, J., Teramoto, T., Chang, Y.F., Nakano, M., Abdelfattah, A.S., Fujiwara, M., Ishihara, T., Nagai, T., and Campbell, R.E. (2011). An expanded palette of genetically encoded  $Ca^{2+}$  indicators. *Science* 333, 1888-1891.